INTRICACIES OF THE 2013 NOVEMBER 3 HYBRID-ECLIPSE WHITE-LIGHT CORONA

JAY PASACHOFF[1,2], VOJTECH RUŠIN[3], METOD SANIGA[3,4], ALLEN B. DAVIS[5,6]
[1] Williams College—Hopkins Observatory, Williamstown, MA 01267-2565, USA; eclipse@williams.edu
[2] Caltech 150-21, 1200 East California Blvd., Pasadena, CA 91125, USA; jmp@caltech.edu
[3] Astronomical Institute, Slovak Academy of Sciences, 05960 Tatranská Lomnica, Slovakia; vrusin@ta3.sk
[4] Institute for Discrete Mathematics and Geometry, Vienna University of Technology, Wiedner Hauptstrasse 8-10, A-1040 Vienna, Austria; metod.saniga@tuwien.ac.at
[5] Astronomy Department, Williams College, Williamstown, MA 01267-2565, USA; abd14@williams.edu
[6] Astronomy Department, Yale University, 52 Hillhouse Avenue, New Haven, CT 06511; allen.b.davis@yale.edu

ABSTRACT

We analyze the structure and dynamics of the white-light corona (WLC) as observed in Gabon during the annular-total ("hybrid") solar eclipse of 2013 November 3 (total across Africa, including our location). The eclipse occurred between the double maxima (2012 and 2014) of cycle 24, which ranks among the weakest in many decades. Even though the cycle amplitude, in terms of sunspot number, was very low, the WLC had a typical cycle maximum shape with many helmet streamers or long rays uniformly distributed around the solar limb and filled with many loops, arcades or thin rays. This distribution yields the flattening index of 0.04, appropriate for its phase of the cycle. We observed two coronal mass ejections (CMEs) and an eruptive prominence during the eclipse. Their positions are rather atypical (far away from active regions): the first is located at position angle (PA) 19º and at a height of 2.7 solar radii (its lower edge was located at 2.13 solar radii). The second was located on the opposite side at PA 196º at a height of 3.90 solar radii. The projected speed of the first CME was approximately 140 km s^{-1}; that of the second CME was about 120 km s^{-1} (these speeds were derived using *SOHO*/LASCO C2 observations, of much lower resolution). Attention is also drawn to a possible relation between the fine structure of the WLC and a dynamic prominence seen above the NE solar limb. Finally, a brief comparison of the WL and EUV coronas is given.

Key words: eclipses – Sun: chromosphere – Sun: corona – Sun: coronal mass ejections (CMEs) – Sun: magnetic fields – Sun: UV radiation

1. INTRODUCTION

Total-eclipse observations of the white-light corona (WLC), photospheric light scattered by free electrons (K-corona) or dust particles above the solar surface (F-corona), remain the best way to study the lower and middle continuum corona in spatial resolution and contrast (Golub and Pasachoff 2010, 2014). The WLC is regularly observed not only from space (e.g., with *SOHO*/LASCO or *STEREO*/SECCHI), but, though not quite at the time of this eclipse, also on the ground with the Mauna Loa Solar Observatory COronal Solar Magnetism Observatory (COSMO) with its K-Coronagraph (Tomczyk, Gallagher, Wu, et al., 2013; Burkpile, 2013) replacing the *Mark-IV K-Coronameter* (Elmore, Burkepile, Darnell, Lecinski & Stanger, 2003); still, observations during total solar eclipses remain unmatched in quality. This advantage is because the eclipse images not only offer much higher spatial resolution, by a factor of over 20, of the WLC structures (e.g., Rušin, Druckmüller, Minarovech & Saniga, 2008; Druckmüller, Habbal and Morgan, 2014; Pasachoff et al., 2015), but they also display structures located up to 2.2 solar radii (1.2 solar radii above the limb) that are still not available from space-borne observations. All prominent coronal structures, including their densities and temperatures, are directly associated with photospheric magnetic

fields/fieldlines, so their study is very important for a deeper understanding of coronal magnetic fields (at present nonmeasurable directly) and properties of the solar wind (its source, speed, density, etc.), as discussed, e.g., by Antiochos (2012 and references therein). Moreover, eclipse observations allow us to study a sort of "direct" connection of the WLC with features in the solar photosphere and chromosphere, and with the EUV or X-ray corona (Lu, Pasachoff, Su, van Ballegooijen, Seaton, et al., 2013). As follows from the recent work by Usoskin et al. (2015), the WLC brightness/structures are also relevant to the study of long-term solar activity.

It is well-known [e.g., Koutchmy (1988), Pasachoff (2009), Druckmüller, Habbal & Morgan (2014), Pasachoff et al. (2015)], that the WLC is a highly structured object on both a large scale (helmet streamers, coronal holes, etc.) and a small scale (polar rays, loops, rifts, etc; see Reale, 2014). Small-scale structures were recognized thanks to new image-processing methods, using sophisticated mathematical procedures (e.g., Druckmüller, Rušin & Minarovjech, 2006; Druckmüller, 2009) to overcome the dynamic-range problem by compositing from dozens of eclipse images. The result of such computer analysis resolves very small brightness/density differences between individual small-scale structures. These methods also allow us to shed a novel light on the connection between prominences (both dense and cool examples) and the hot and tenuous WLC (e.g., Habbal et al., 2010). All this recent knowledge implies that a classical picture of the solar corona as a static and symmetric single object has to be abandoned and that the WLC is, rather, a bunch of a variety of autonomous structures generated and bound together by magnetic fields, and with motions visible over the hours that the umbra takes to cross the Earth (e.g., Pasachoff, Rušin, Druckmüllerová, Saniga, Lu, et al. 2011; Pasachoff, Rušin, Druckmüllerová, Saniga & Babcock, 2011; Pasachoff, Davis, Demianski, Lucas, Lu, et al., 2013; Pasachoff, Davis, Demianski, Lucas, Lu, et al., 2014; Pasachoff, Davis, Demianski, Rušin, Saniga, et al., 2014; Pasachoff, Lu, Davis, Demianski, Rušin, et al., 2014).

2. OBSERVATIONS AND OBSERVATIONAL SITES

The hybrid solar eclipse on 2013 November 3, began in the Atlantic Ocean (with only the beginning as annular) and continued as a total eclipse over most of the Atlantic Ocean and then over Africa, from Gabon to Ethiopia. The path of the shadow was very narrow, around 30 km wide in Gabon and only 16 km wide in Ethiopia, where sunset was observed during totality; the length of totality in Gabon on the central line was 1 minute and 7 seconds at an altitude of 43°, compared to only 16 seconds in Ethiopia at the sun's elevation of only 16º (Espenak, 2013; Jubier, 2013). Although meteorological predictions and travel conditions were not very favorable and duration of the eclipse was relative short, several eclipse teams visited Gabon, Uganda, Kenya and Ethiopia.

Our international team (the Williams College Expedition) observed the WLC with different focal-length lenses (200 – 800 mm) in central Gabon just outside La Lopé National Park. We took many images with exposure times from 1/2000 to 8 s, using Nikon and Canon DSLRs cameras. Our main observational site was in the small village of Mkongo 2, located in the forest just to the east of the national park, an hour's drive south of the park's Lodge; to maximize the chance of avoiding clouds, we had a secondary site located 7 km north of Mkongo 2. The Sun was briefly covered by thin clouds around 30 minutes before second contact but the sky cleared well before totality. Coordinates for the main site are: 0º17.63' S at 11º 45"23' E, duration 59 s, observation time: 13:55:41 – 13:56:40 UT, with solar elevation above the horizon: 43º. The sky was completely blue (following a brief downpour during the early partial phase) during the total phase of the eclipse, with some clouds visible near the Sun on long exposures. The general shape of the WLC, processed by Druckmüller's method, is shown in Figure 1.

Figure 1. The WLC as observed on 3 November 2013 at Mkongo 2 (alongside La Lopé National Park in Gabon) from our eclipse data processed by Druckmüller's method. (J. M. Pasachoff, A. B. Davis, V. Rušin and M. Druckmüller).

3. RESULTS

3.1. Large-scale structure of the WLC

As is generally known, the large-scale WLC, dominated by helmet streamers, varies with the phase of the solar-cycle. Helmet streamers around the cycle minimum are distributed near the equator or just above it, while the polar regions are occupied by coronal holes – coronal features with relatively low density and temperature and open field lines, filled with polar plumes (also known as polar rays). (See Pasachoff et al., 2008, about the 2006 eclipse.) On the other hand, there are many helmet streamers - outstanding coronal structures/features, known since the very beginning of eclipse solar-corona research, distributed nearly uniformly around the solar limb (circularly symmetric) around/in cycle maximum. Polar plumes are then absent or invisible. Helmet streamers, between solar maximum and minimum, are located at different position angles, but are usually connected to a distribution of quiescent prominences. As recently shown by Rušin, Saniga & Komžík (2013), the typical width of a helmet streamer located above the neutral line that separates opposite polarities of the large-scale magnetic fields is around 32°, irrespective of the cycle magnitude, cycle phase, or the strength of solar magnetic fields. But neutral lines follow distributions of quiescent prominences that migrate over a cycle, so the same is valid for helmet streamers, e.g., Bělík, Marková, Rušin & Minarovjech (2004). However, distributions of helmet streamers within different cycles also depend, as shown by Waldmeier (1963), on the position of stationary prominence zones, whose arrival near the poles correlates with sunspot number (recently restudied by Clette and Lefèvre, 2015) and differs between high and low magnitudes of the cycle. At that time it was, however, not known that such zones are a part of a larger phenomenon now called large-scale meridional flows, e.g., Upton and Hathaway (2014). We note that the lifetime of helmet streamers is not known. Figure 1 confirms that the 2013 November 3 WLC was of a maximum type, as expected. The eclipse occurred shortly before the cycle maximum (double peaked, around January 2012 and March 2014, with northern-hemisphere maximum first and southern-hemisphere maximum following over two years later), according to the smoothed monthly values of sunspots (http://www.swpc.noaa.gov/products/solar-cycle-progression or http://sidc.oma.be/silso/).

To express the shape of the WLC, Ludendorff (1928) introduced the term "ellipticity." (See also Golub and Pasachoff, 2010.) The Ludendorff flattening coefficient is a measure of deviation of the WLC isophotes from the shape of a circle that varies with the height of the isophote above the solar surface. Usually, the ellipticity, or flattening index (epsilon = a + b), is defined for the height of 2 solar radii and is obtained from the linear course of the straight line with coefficients a,b (Waldmeier, 1970). The flattening index over the last 150 years (Pishkalo, 2011) varied between 0.0 (cycle maximum) and 0.35 (cycle minimum). The flattening index for the 2013 eclipse now under study (see Figure 2) amounts to 0.04 (Rušin, Saniga & Komžík, 2014) and fits well into the relationship found by Pishkalo. We note that although the average value of the solar polar magnetic field strength in cycle 24 was about one half of that in cycles 22 and 23, the flattening index of the WLC does not seem to reflect this fact.

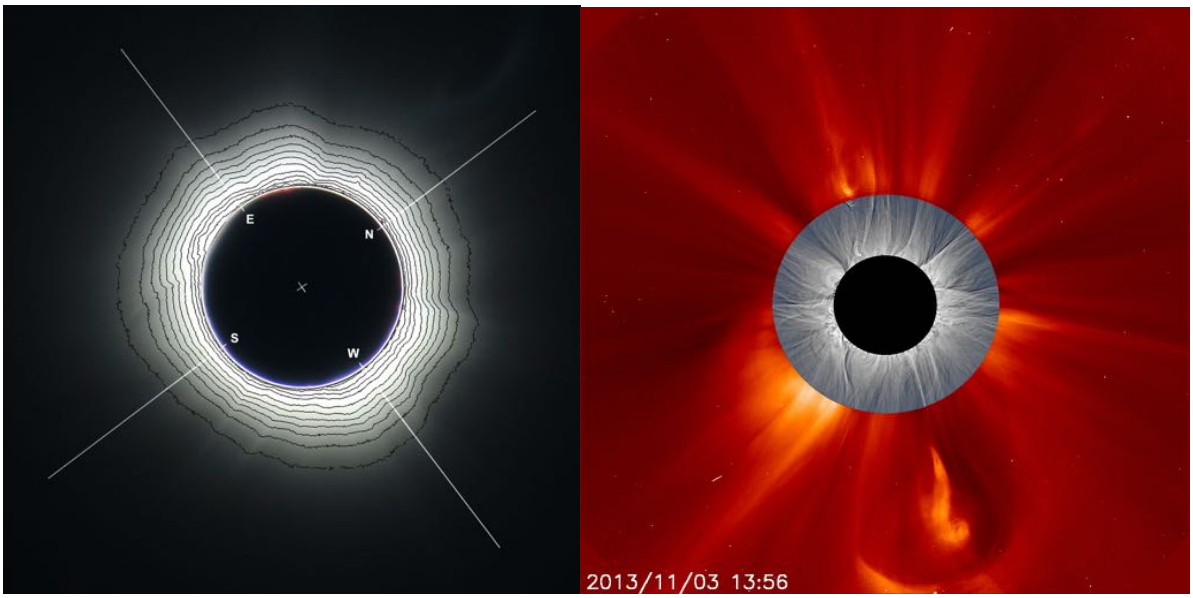

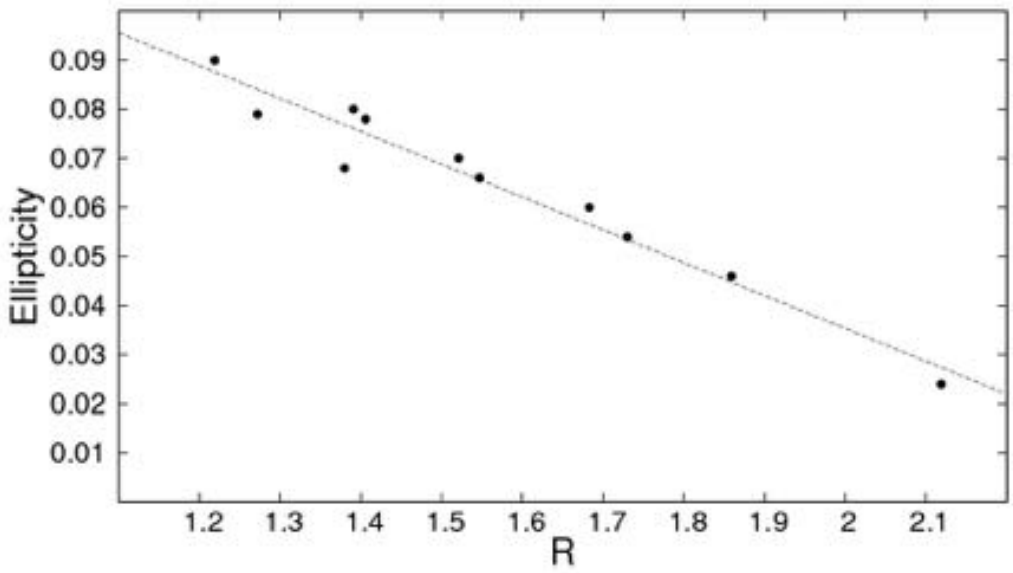

Figure 2. (*Top left*) Isophotes of the WLC as observed at Mkongo 2 and processed by M. Druckmüller. (*Top right*) A composite of a *SOHO*/LASCO image and our processed eclipse WLC image. (*Bottom*) The ellipticity of the WLC where a = – 0.0669 and b = 0.1692; the distance *R* is given in solar radii.

Figure 1 illustrates the complicated structure of the WLC quite well. Large-scale structures are filled with many small-scale structures, like thin rays and loops (both bright and dark). We shall deal first with helmet streamers, which are also seen in SOHO/LASCO C2 images, such as the one shown in Figure 2 (top right).

A classical helmet streamer with a prominence located at its base and accompanied by an aggregate of dark and bright loops above the prominence is seen at PA 43°–73° (its center at PA 58°) and PA 138°–170° (its center at PA 156°). One is tempted to assume that these streamers have their foot-points rooted at the opposite sides of large-scale magnetic fields. Although distributions of neutral magnetic field-lines as measured by Stanford magnetograms are not available for the day of observation, the corresponding data for the day before and after seem to support this conjecture. Other bases of helmet streamers can be seen at PA 78°–104° (centered at PA 90°), PA 249°–285°, PA 288°–313° (twins with tiny prominences at PA 284° and PA 308°), PA 313°–343° and at PA 352°–25° (prominences at PA 358°). We note that helmet streamers as indicated above are created with many outlines of streamers and, it is, an effect of helmet streamers distributed along the line of sight (see, e.g., Figure 3 in Rušin, Saniga & Komžík, 2013). Moreover, some of these streamers are considerably curved with height and it is thus not straightforward to guess their prolongation from *SOHO*/LASCO images to the solar limb. Finally, helmet streamers seen in PA 38°–44° and PA 73°–78° are separated by a conspicuous void.

3.2. *WLC small-scale structures*

As it is obvious from Figure 3, the small-scale structure of the WLC is also rich and complex. We can see that a number of prominence jets (which, of course, we see from their H-alpha emission and therefore look reddish on the images) continue as prolongations. This point agrees with the conclusion of Habbal, Morgan & Druckmüller (2014) that the unraveling of prominences and the outward expansion of the helical twisted field lines linked to them could be the solar origin of twisted magnetic flux ropes detected in interplanetary space, and that this is the mechanism by which the Sun sheds its magnetic helicity. It is not unlikely that the prominence-corona interface could serve as a source of the slow solar wind. Moreover, our pictures also feature so-called trans-equatorial loops (indicated in the figures by arrows), rooted at PA 70° (the northern hemisphere; no sunspot groups) as well as at PA 98° (the southern hemisphere; a few sunspots in their vicinity). Such trans-equatorial loops are surmised to play a very important role for three major solar phenomena: dynamo, reconnection, and eruptions, as discussed by Pevtsov (2004).

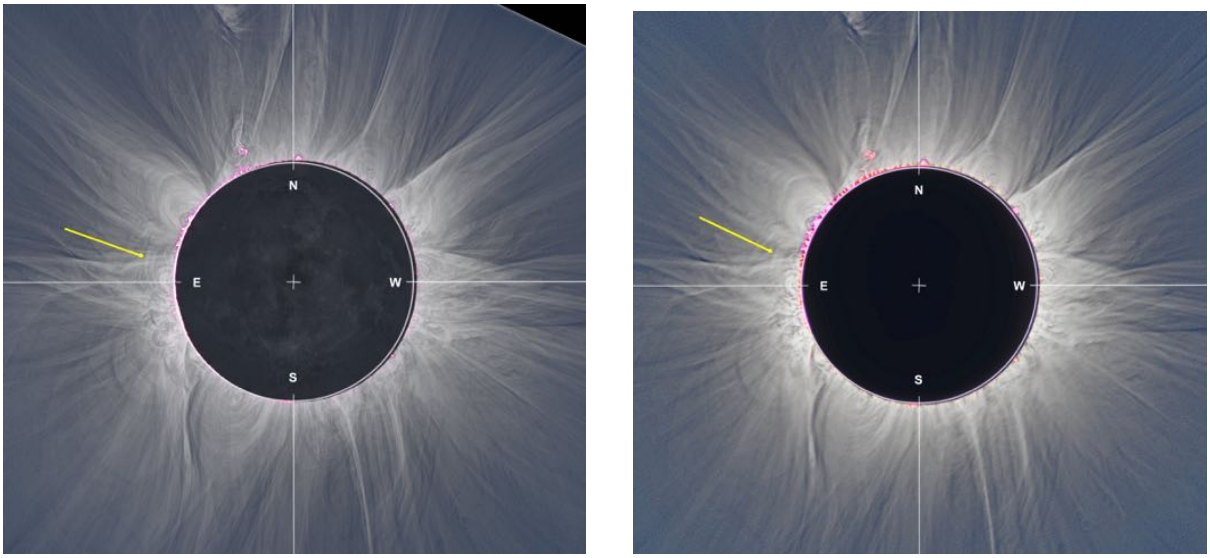

Figure 3. Small-scale structures of the 2013 WLC from observations in (*left*) Lambarene, and, 3 minutes later (central time of totality), (*right*), Mkongo, including trans-equatorial loops, marked by a yellow arrow. Pink-colored areas correspond to prominences. (Credit:

(*left*) Emmanoulidis, processed by Druckmüller, (*right*) Pasachoff, Rušin, Davis; also processed by Druckmüller).

3.3. Coronal mass ejections

CMEs, together with flares, are regarded as the most energetic manifestations of solar activity and their ejection is one of the key mechanisms by which the solar magnetic fields are restructured. CMEs inject large quantities of mass and magnetic flux into the heliosphere, causing major transient disturbances, e.g., Webb and Howard (2012), so they are interesting not only for solar research, but for technological reasons as well for the safety and security of communication satellites and terrestrial power lines, for example. Most CMEs are believed to result from flares, eruptive prominences, and/or magnetic-field reconnection (e.g., Webb and Howard (2012) and references therein). Although their occurrence during a very short interval of total eclipse observed from one spot on Earth—or during the 2 hours or so during which the umbra traverses the Earth—is more or less a matter of luck, such eclipse CMEs have nevertheless been observed within the past few years, like a CME during the 2012 November 13/14 eclipse (Pasachoff et al., 2015). The eclipse "comets" reported in the past (Cliver, 1989; Olson and Pasachoff, 1998) may well have been CMEs seen long before the phenomenon was appreciated.

The November 2013 eclipse is unique in history in the respect of CMEs, as it was accompanied by two different CMEs, both lying far away from active regions and on opposite sides. The first CME, centered at 2.83 R_S (and based at 2.17 R_S), was seen at PA 11° (Figure 4). It looks like a prolonged bubble with open top and does not seem to be visibly anchored to the solar surface. Its vicinity is characterized by a number of threadlike streamers that seem to “emanate” from the region located at PA 26°, the latter being a host of several prominences. This CME is likely to be related to a small prominence, one of whose legs is anchored at PA 25°. Although the upper part of this prominence exhibited slight dynamical behavior in visible light at the time of the eclipse, it did not show any pronounced expansion in the He II line observed from *SDO*. Projected speed of this CME as derived from *SOHO*/LASCO C2/LASCO C3 observations is estimated to be around 140 km s^{-1} (at 23:54 UTC, the CME was observed with LASCO C3 at the height of around 11 R_S). Assuming that this speed was constant, we infer the onset time as occurring about 10:55 UTC; this assumption, however, does not seem realistic as the above-mentioned slow evolution of the ambient prominence took place, as inferred from *SDO*/AIA observations, since at least 06:14:00 UTC.

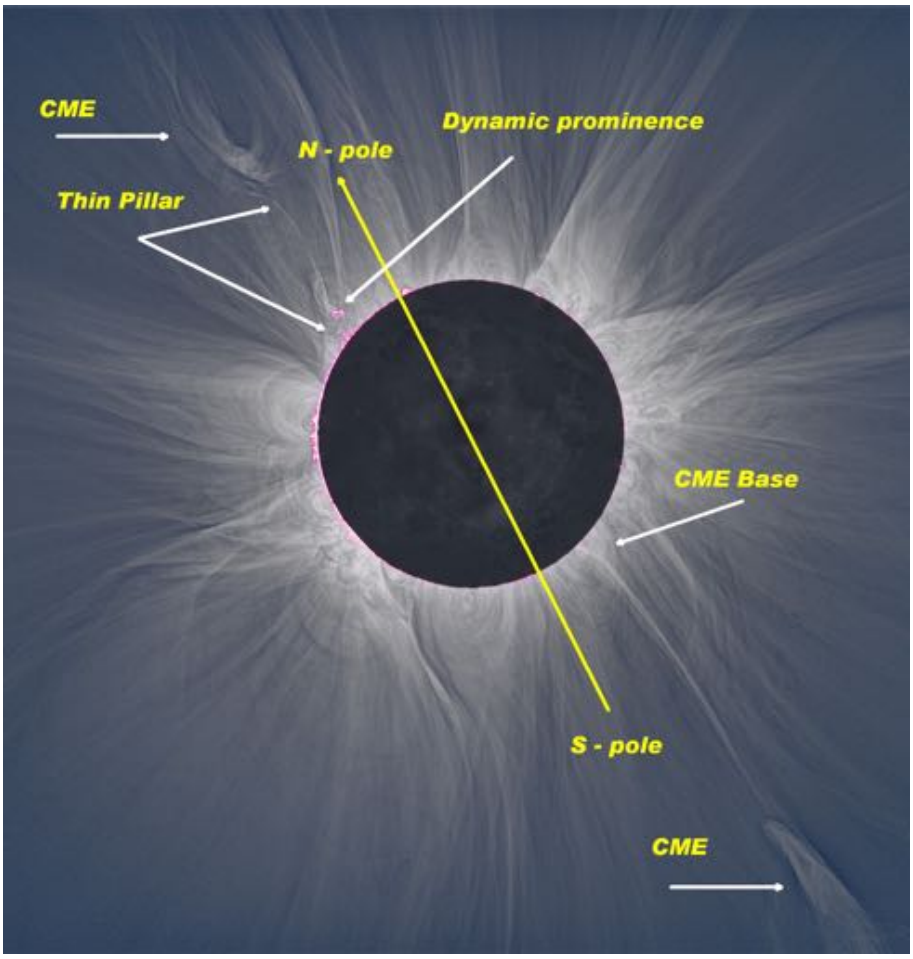

Figure 4. The northern CME and its rather intricate neighborhood; note a remarkably-prolonged thin pillar and an adjacent prominence. (Background-image credit: Emmanoulidis & Druckmüller)

The other CME (see Figure 5) is located at PA 192°, having its base at 3.26 R_S and its upper part at about 5.2 R_S. Although appearing as a compact object from *SOHO*/LASCO C2, its visible structure—given the 20-times-better resolution of the Druckmüller reductions—is complex, featuring a bright, hook-shaped core part and a bright outer shell, characteristic for a mature CME. The inner part is located close to the end of a coronal ray based at PA 197°, the site of a not-well-defined prominence (see Figure 5). A more detailed inspection of Figure 4 indicates that this ray looks like an entanglement/projection of several spiral-like rays linked to a system of concentric loops at PA 196°–200°. The upper part of the core exhibits also a screw-like form (see Figure 6).

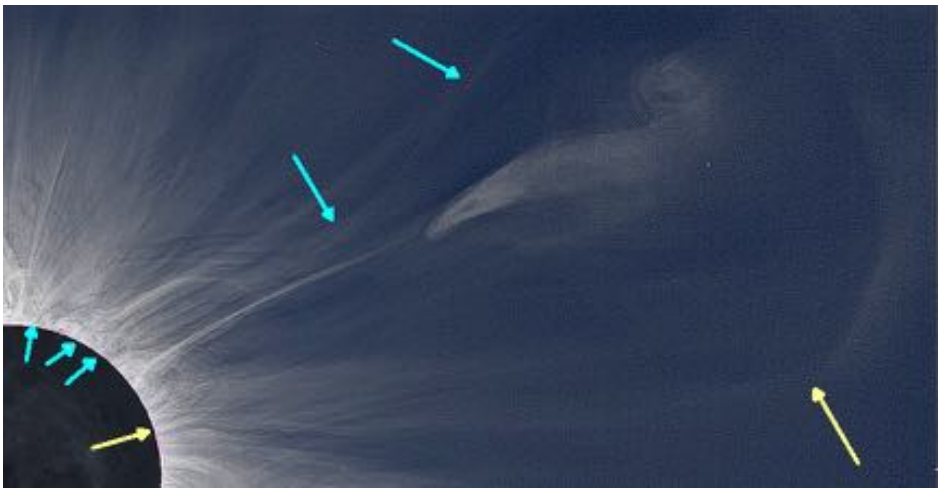

Figure 5. The southern CME located at PA 192°. Arrows indicate outer loops with a possible connection to coronal structures in the lower corona. (background-image credit: Emmanoulidis & Druckmüller).

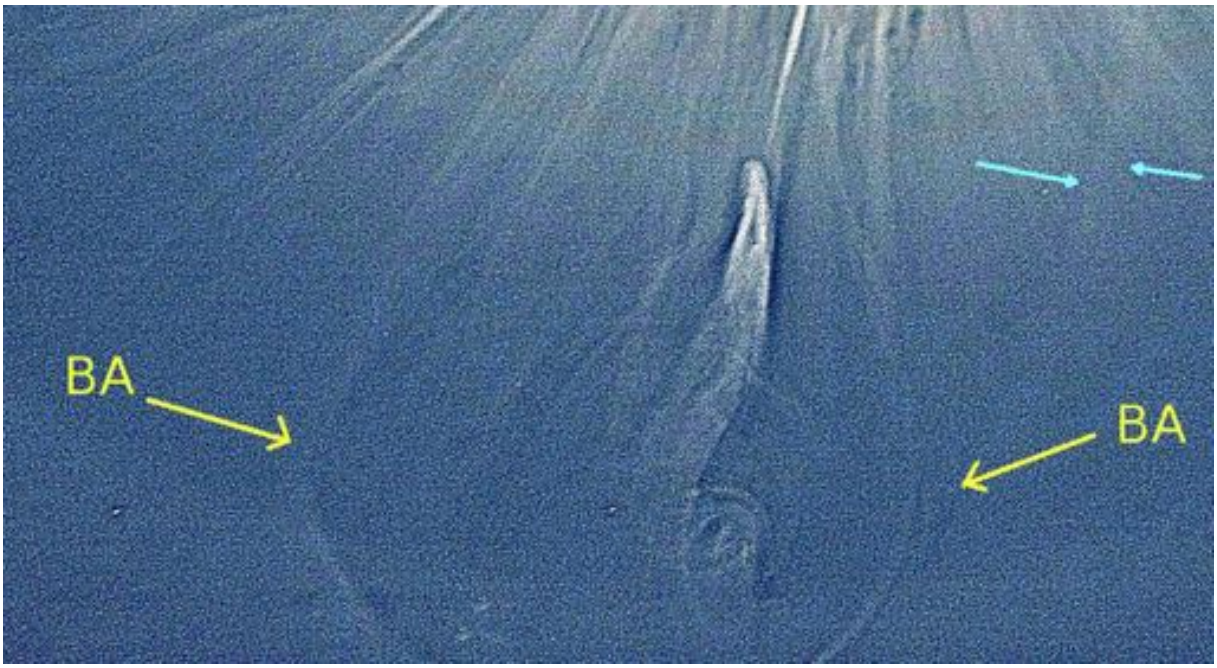

Figure 6. Detail for the southern CME. BA denotes a bright arcade/shell rooted at different PAs of a leg of ejected material. Blue arrows point out a tiny coronal arcade.

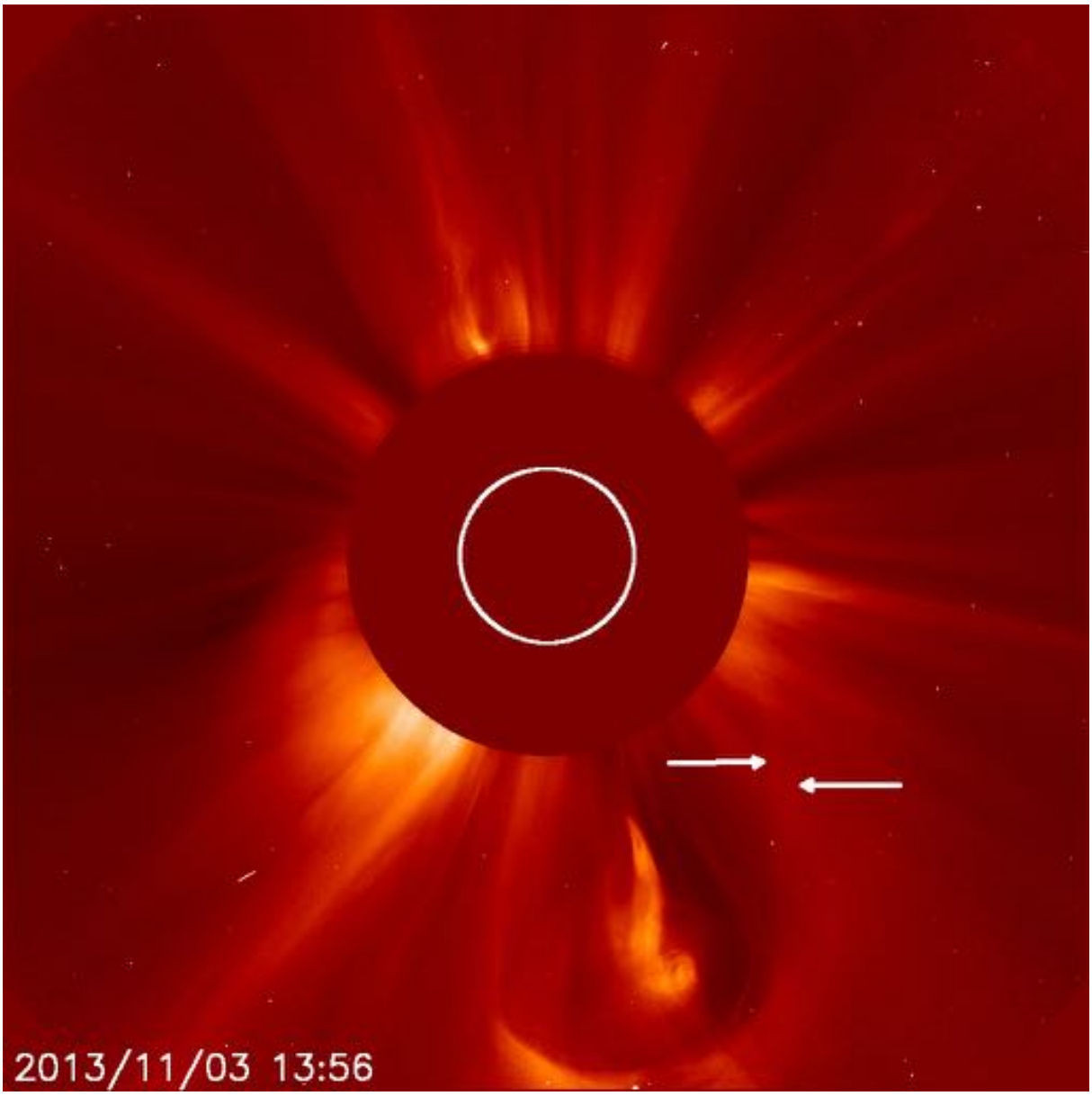

Figure 7: (*a*) The position of the outer shell (indicated by white arrows) of the southern CME, as observed with *SOHO*/LASCO C2, at a resolution about 20 times lower than that of our reduced eclipse images. A related image, including also a nearly simultaneous SWAP image of coronal gas on the disk, appeared as Astronomy Picture of the Day on 2013 November 11: http://apod.nasa.gov/apod/ap131111.html.

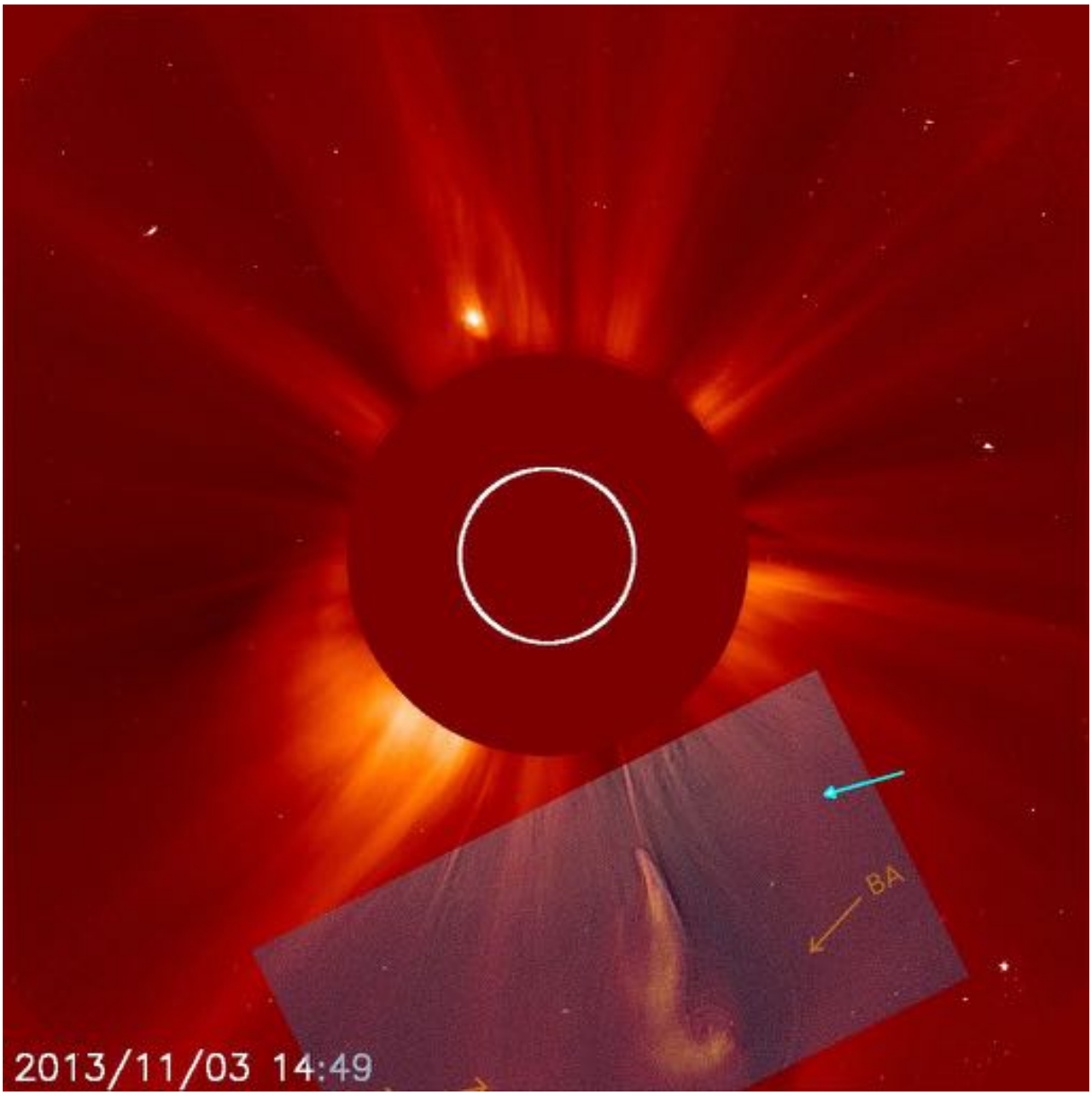

(*b*) An overlay of the eclipse WLC (rectangular inset) on the *SOHO*/LASCO image. The northern part of the arcade is well discernible in both the images.

Concerning the structure of the outer bright shell/arcade of this CME (see Figure 7), its northern leg is likely to be rooted in the area around PA 216°–225°, or PA 242° at the highest (indicated by blue arrows in Figure 5), whilst its southern leg at about PA 186°. Projected speed of this CME as derived from *SOHO*/LASCO C2 between 13:56 and 15:00 UTC is estimated to be around 175 km s^{-1} – for the internal, brightest part of the CME, supposed to be a part of a prominence. From *SOHO* observations, we derived a projected radial speed for this arcade between 08:12 and 13:56 of around 120 km s^{-1}. *SOHO*/LASCO C3 observations of this complex showed its top at 23:54 at the height of 26 R_S (the arcade; the prominence part was a bit lower – at 18 R_S). Assuming constant speed, we estimate the onset of this CME as 06:30 UT, a little bit earlier than that of the other CME. The difference in speeds may well be ascribed to the fact that the inner part kept "disentangling" with the height, so it was difficult to trace downward the path of one-and-the-same object.

It is natural to ask at this point what triggered these CMEs, and whether the two could have originated from the same source. As already mentioned, both CMEs were observed far

from active regions, whose locations are depicted in Figure 8, as if they were located almost at the opposite ends of a huge magnetic field line. These facts imply that the eruptive nature of the CMEs is quite plausible, in particular for the southern CME. Its adjacent prolonged prominence with longitudinal mass transfer was at 06:43:56 UT situated above the south pole, yet at 06:58:32-07:14:32 UTC it dramatically changed its shape, its left part remaining more or less the same but its middle and right parts disappearing, as illustrated by observations from *SDO*/AIA (Figure 9). Such a change is strange behavior for eruptive prominences, as these features usually start slowly, followed by a rapid expansion (e.g., Rušin and Rybanský (1982); see also Webb and Howard (2012) and Chen (2011) for discussions of various types of CMEs and their models).

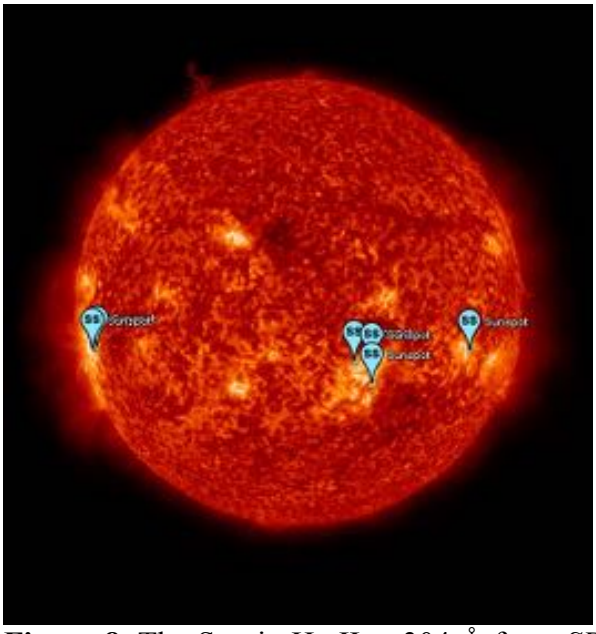

Figure 8. The Sun in He II at 304 Å from *SDO*/AIA. Active regions on the solar surface are marked. (NASA/*SDO*/AIA/)

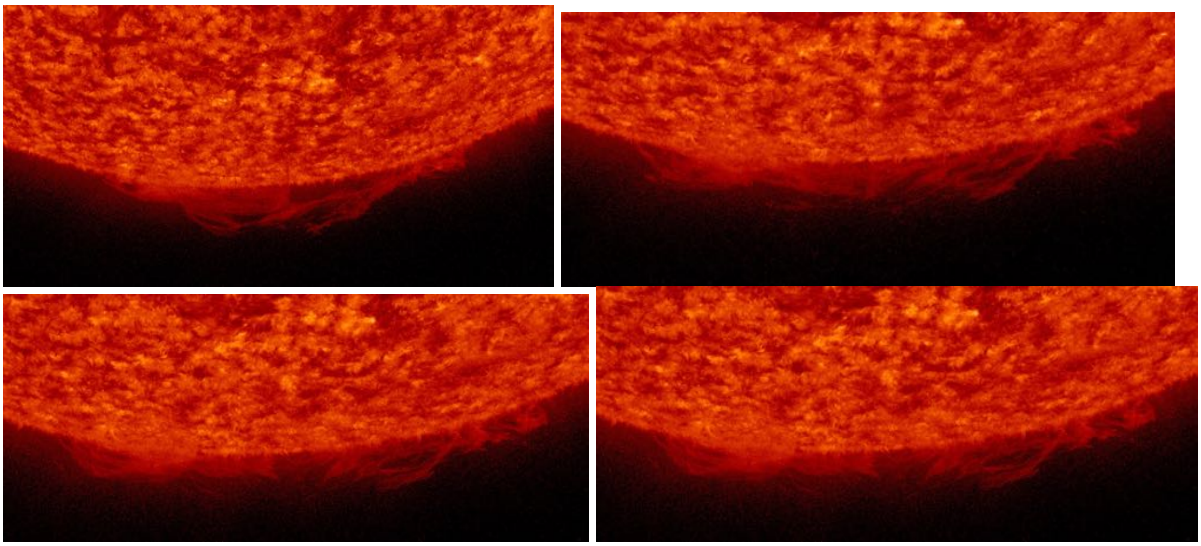

Figure 9. The prominence over the south pole at 06:14:20 UTC (*top left*), 06:58:32 UTC (*top right*), 07:14:32 UTC (*bottom left*) and 07:30:08 UTC (*bottom right*). The intervals are, therefore, 44 min, 16 min, and 26 min, respectively. (NASA/*SDO*/AIA)

4. THE WHITE-LIGHT AND EUV CORONAS

Nowadays, during total solar eclipses one can observe from the ground not only the WLC but also–using narrow-band filters –the emission corona in forbidden lines of the visible part of solar spectrum (see, e.g., Habbal et al., 2010, and/or Rušin et al., 2010). In addition, we have at our disposal space-borne (*SOHO*, *PROBA2*/SWAP, SDO/AIA) observations of the EUV corona in a number of spectral lines. As no terrestrial observations in forbidden lines were available for the day of the eclipse, to compare the WL and EUV coronas we examined *SDO*/AIA space observations in the lines of 171 Å (Fe IX and Fe X) at temperatures of about 1 MK and 131 Å (Fe XX and Fe XXIII) at temperatures of about 10 MK (Figure 10).

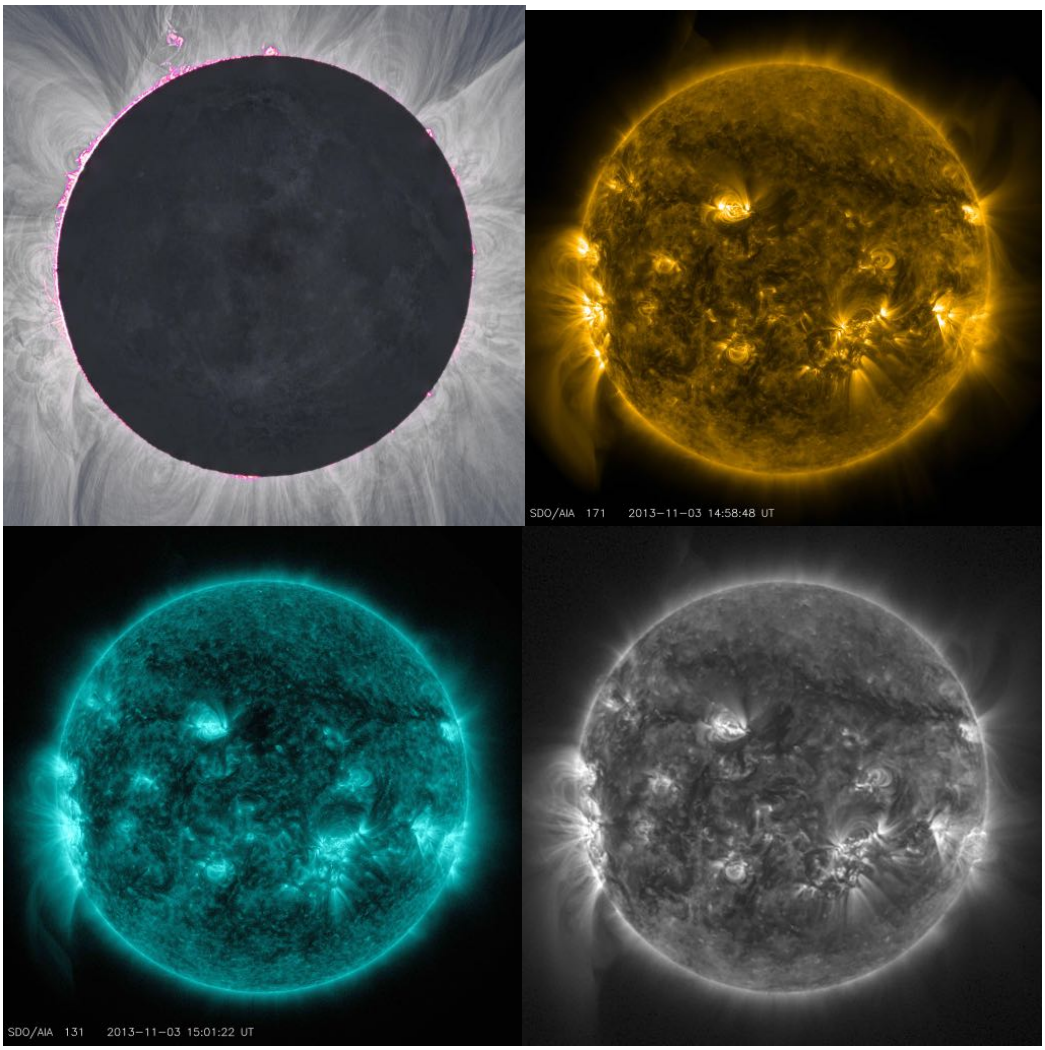

Figure 10. Fine structure of the WLC (*top left*) compared with that of the EUV corona in 171 Å (*top right*) and 131 Å (*bottom left*) from *SDO*/AIA, as well as with the *PROBA2*/SWAP image (*bottom right*). Solar north is up.

Even a passing look at Figure 10 shows that while the loops of enhanced emission of the EUV corona are uniquely tied to active regions, in the WLC such loops are observed around the whole solar limb. In order to spot finer differences between the two coronae, we present a composite image of the WL and EUV 171 Å corona (Figure 11) as well as that of the WL and EUV 131 Å corona (Figure 12); the stronger the yellow/green color, the stronger is the emission in the corresponding area. Here it is worth mentioning that a rather darker WLC area between two helmet streamers at the western limb appears quite bright in both EUV coronae.

It is natural to ask why the loops of both coronae coincide only around active regions and: Can this fact be ascribed only to high temperature and density? Since the WLC was in the forbidden lines of the visual spectrum observed only in the regions occupied by coronal condensations (density greater than 10^{10} cm^{-3} and temperature above 5×10^{6} K), does it mean that the temperature of the WLC in the areas of absent EUV emission is less than usually assumed? What is the limiting value of plasma density for the WLC to be visible/observable?

Given the frequent occurrence of dark voids in the WLC, is the main agent behind the solar wind only the high temperature of the corona (Parker, 1958) or are there other mechanisms behind (for a recent discussion, see Habbal, Morgan & Druckmüller, 2014)?

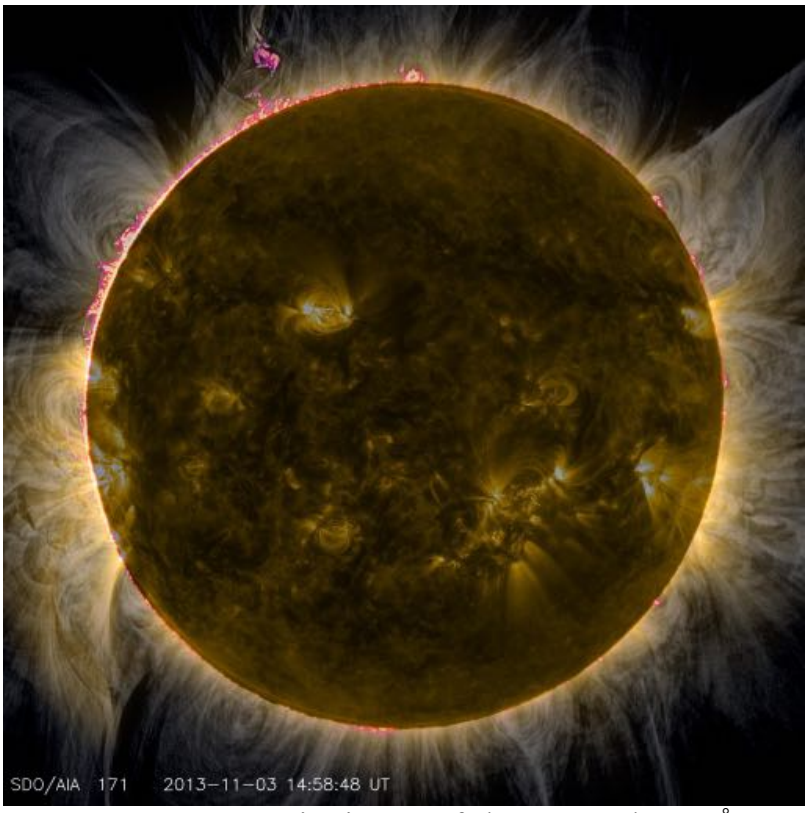

Figure 11. A composite image of the WL and 171 Å EUV coronae. The strength of the yellow color corresponds to the strength of the emission in the corresponding area.

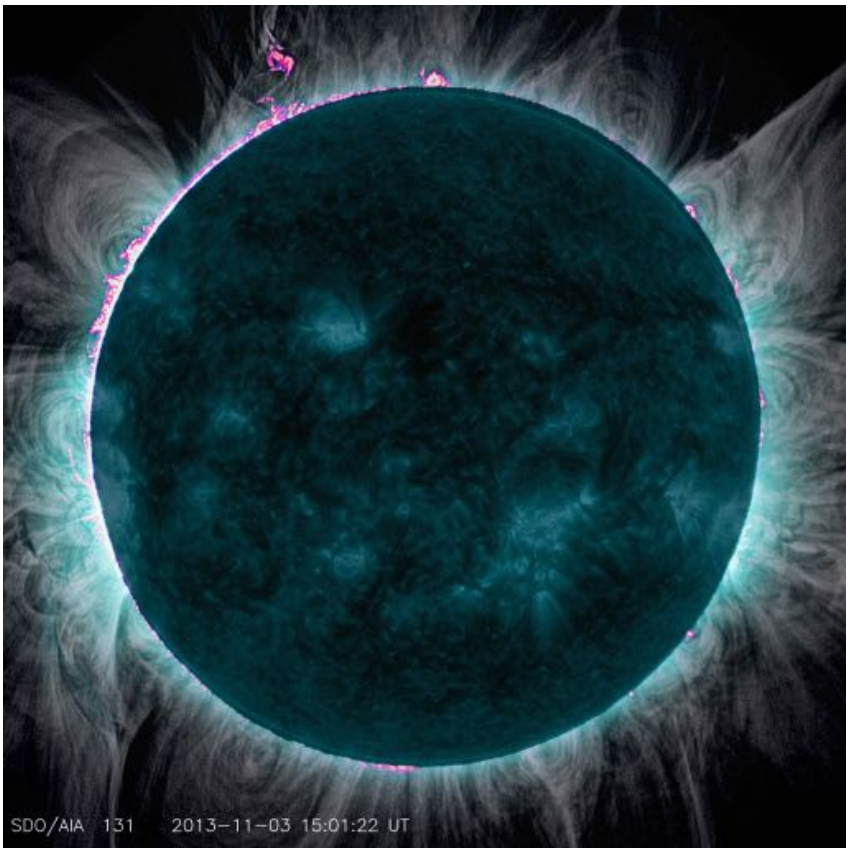

Figure 12. A composite image of the WL eclipse and 131 Å EUV coronae. The strength of the green color corresponds to the strength of the emission in the corresponding area.

5. DISCUSSION AND CONCLUSION

The large-scale structure of the WLC of the 2013 November 3 total eclipse, being dominated by helmet streamers and radial plumes/rays, is of maximum type with flattening index 0.04. On small scales, one sees a number of bright loops and arcades, some being trans-equatorial. Despite the fact that the averaged strength of solar global magnetic fields, as measured at the *Stanford Solar Observatory* (http://www.solen.info/solar/polarfields/polar.html), is only a half that in the previous cycles, this large-scale WLC has no pronounced deviation from the previous ones of the same cycle phase. A remarkable feature is the near-simultaneous occurrence of two CMEs located on the opposite ends of the solar disk and far away from active regions. Both CMEs seem to be the result of the ejection of mass from prominences rather than from the upper corona, as in the cases discussed by Webb and Howard (2012) and/or Pasachoff et al. (2015). Comparing the structure of the WLC with that of the EUV corona in the two different lines discussed above confirms earlier findings that these agree only near active regions. Hence, the question remains open whether the temperature of the WLC is (much) lower than generally accepted.

The coronal loops and narrow threads that we observe at the high resolution available in this region of the corona uniquely from the ground during total eclipses, some 20 times higher resolution than is available from *SOHO*/LASCO C2 for the overlapping region, are the building blocks of the solar corona. As such, they are important for being basic laboratories to investigate the mechanisms of coronal magnetism, coronal dynamics, coronal heating, global structure, and the solar wind. Ground-based observations of the WLC with both higher spatial and temporal resolution, in the umbra along the full duration of the eclipse across the

Earth's surface, hereby show their justification. As was recently shown by Hudson (2015), there is a connection between high-energy (TeV) cosmic rays as measured by *RHESSI* and the Sun: particles when approaching the Earth can be deflected by solar magnetic field, and this deflection obviously depends upon the coronal magnetic field in a direct way.

In light of all that, we look forward to the crowdsourced US Eclipse 2017 Megamovie project (Hudson, McIntosh, Habbal, Pasachoff & Peticolas, 2011; Pasachoff, 2015; eclipsemegamovie.org) and the Citizen Continental America Telescopic Eclipse Experiment (Citizen CATE; Penn, Baer, and Isberner, 2015) with its 61 identical telescopes/CCD-systems at a 1-s cadence over a 90-minute interval that would be the first time since the *Concorde* observations of the 1973 eclipse (Beckman, Begot, Charvin, et al., 1973) that a solar eclipse has been continuously tracked with high time resolution for a period longer than the duration of totality at a single location, though several of our eclipse articles (such as Pasachoff, Rušin, Druckmüller, et al., 2008, 2009) discuss intermittant observations, even over an hour in duration. We thus hope for continuous monitoring of coronal evolution and dynamic activity, including variations in the low corona, and also capturing associated prominence systems at high (spatial and temporal) resolution for an extended period of time.

This work was partially supported by the National Geographic Society's Committee for Research and Exploration, under Grant 9321-13, "Total Solar Eclipse in Gabon at Sunspot-Cycle Maximum," and the VEGA (SAV) grant 2/0003/13. We thank Xavier Jubier for creating and maintaining the software *Solar Eclipse Maestro*, which we used to control several of our cameras. We also thank Miloslav Druckmüller for his expert work in creating the composite images seen here, and Constantine Emmandoulidis for his expert photography We are grateful to Matej Sekeráš his help with a careful relabeling of several figures.

We thank Michael Zeiler (eclipse-maps.com) for his expert mapping and GPS locating ability, Polly White for measuring temperature on site and various assistance, Zophia Edwards '05 for logistic assistance, and Michael Kentrianakis for collaboration on imaging, logistics, and communications. We thank Patrice Okouma of Nommo Astronomia (Gabon) and the South African Astronomical Observatory for his organization and assistance. We thank His Excellency Michael Moussa-Adamo, Ambassador Extraordinary and Plenipotentiary of the Gabonese Republic to the United States of America and Dr. Mireille Obama Nguema E. Moore of the Gabon Embassy in Washington; Etienne Massard K. Makaga and Aboubakar Mambimba Ndjoungui of AGEOS, the Gabon Space Agency, for their logistics assistance; M. Tchemambela and Lee White of the Gabon National Parcs Agency; M. Michel Flavien Yenot of the Gabon Ministry of Communication; Dante Paradiso, Kevin K. Krapf, and colleagues of the U.S. Embassy in Libreville; Mark Sood of A Classic Tours Collection for travel assistance; and Joel Parriott, then AAS Director of Public Policy, for linking us to the Embassy in DC.

REFERENCES

Antiochos, S. K., Linker, J. A., Lionello, R., Mikić, Z., Titov, V., & Zurbuchen, T. H., 2012, SSRv, **172**, 169 2012SSRv..172..169A, 10.1007/s11214-011-9795-7

Beckman, J., Begot, J., Charvin, P., Hall, D., Lena, P., Soufflot, A., Liebenberg, D., & Wraight, P. 1973, "Eclipse Flight of Concorde 001," *Nature*, **246**, 72 1973Natur.246...72B

Bělík, M., Marková, E., Rušin, V. & Minarovjech, M. 2004, *Sol. Phys*., **224**, 269

Burkepile, J., deWijn, A., Tomczyk, S., Sewell, S., Gallagher, D., Sutherland, L., Card, G., Lecinski, A., Larson, B., Nelson, P., Huang, P., Kolinsky, D., Sitongia, L., Stueben, A., & Berkey, B., 2013, "The COSMO K-Coronagraph," EGU General Assembly 2013, EGU2013-11810 013EGUGA..1511810B

Chen, P. F. 2011, "Coronal Mass Ejections: Models and Their Observational Basis," *Living Rev. Solar Phys*., 8, lrsp-2011-1. URL (accessed 17 August 2011): http://www.livingreviews.org/lrsp-2011-1

Clette, F., and Lefèvre, L. 2015, "The new Sunspot Number: re-calibration, re-computation and implications for the solar cycle," IAU General Assembly, Meeting #29, id.2256393

Cliver, E. W. 1989, "Was the Eclipse Comet of 1893 a Disconnected Coronal Mass Ejection," *Solar Phys*., **122**, 319.

Druckmüller, M., Rušin, V., & Minarovjech, M. 2006, *Contributions Astron. Obs. Skalnaté Pleso (CAOSP)*, **36**, 131-148

Druckmüller, M. 2009, *ApJ,* **706**, 1605
DOI: 10.1088/0004-637X/706/2/1605

Druckmüller, M., Habbal, S. R., & Morgan, H., 2014, *ApJ*, **785**, 14 (7 pp)
doi: 10.1088/0004-637X/785/1/14

Elmore, D. F., Burkepile, J. T., Darnell, J. A., Lecinski, A. R., & Stanger, A. L. 2003, *Proc. SPIE*, 4843

Espenak, F. 2013, *Observer's Handbook: 2013* (Royal Astron. Soc. Canada)

Golub, L., and Pasachoff, J. M., 2010, *The Solar Corona*, 2nd ed. (Cambridge U. Press).

Golub, L., and Pasachoff, J. M., 2014, *Nearest Star: The Surprising Science of Our Sun*, 2nd ed. (Cambridge U. Press).

Habbal, S. R., Druckmüller, M., Morgan, H., Scholl. I, Rušin, V., Daw, A., Johnson, J., Arndt, M. 2010, *ApJ*, 719, 1362
DOI: 10.1088/0004-637X/719/2/1362

Habbal, S. R., Morgan, H., & Druckmüller, M. 2014, *ApJ*, 793, 119, 18 pp. (2014)
DOI: 10.1088/0004-637X/793/2/119

Hudson, H. 2015,
http://sprg.ssl.berkeley.edu/~tohban/wiki/index.php/High_Energies_in_the_Inner_Heliosphere), eclipsemegamovie.org

Hudson, H. S., McIntosh, S. W., Habbal, S. R., Pasachoff, J. M., & Peticolas, L. 2011, The U.S. Eclipse Megamovie in 2017: a white paper on a unique outreach event, arXiv: 1108.3486

Jubier, X., 2013,

http://xjubier.free.fr/en/site_pages/solar_eclipses/xSE_GoogleMap3.php?Ecl=+20131103&Acc=2&Umb=1&Lmt=1&Mag=1&Max=1&Map=ROADMAP

Koutchmy, S. 1988, in *Solar and Stellar Coronal Structures and Dynamics, A Festschrift in Honor of Dr. John Evans*, R.C. Altrock, Ed., National Solar Observatory/Sacramento Peak, Sunspot, New Mexico 88349, p. 208-235.

Lu, M., Pasachoff, J. M. Su, Y., van Ballegooijen, A., Seaton, D. B., & West, W. 2013, "Observations and Modeling of Solar Coronal Structures Using High-Resolution Eclipse Images and Space-based Telescopes with Wide Field of View," AAS SPD, Bozeman. 2013SPD....44...25L

Ludendorff, H. 1928, *Sitz. Ber. Preuss. Akad. Berlin*, 16, 185

Olson, R. J. M., and Pasachoff, J. M. 1998, *Fire in the Sky: Comets and Meteors, the Decisive Centuries, in British Art and Science* (Cambridge University Press).

Parker, E. N. 1958, *ApJ*, **128**, 677
DOI: 10.1086/146580

Pasachoff, Jay M., Vojtech Rušin, Miloslav Druckmüller, Hana Druckmüllerová, Marcel Bělík, Metod Saniga, Milan Minarovjech, Eva Marková, Bryce A. Babcock, Steven P. Souza, and Jesse S. Levitt, 2008, "Polar Plume Brightening During the 29 March 2006 Total Eclipse," *ApJ*, **682**, 638

Pasachoff, J. M. 2009, "Solar Eclipses as an Astrophysical Laboratory," *Nature*, **459**, 789

Pasachoff, J. M., Rušin, V., Druckmüller, M., Aniol, P., Saniga, M., & Minarovjech, M. 2009, "The 2008 August 1 Eclipse Solar-Minimum Corona Unraveled," *ApJ.* **702**, 1297

Pasachoff, J. M., Rušin, V., Druckmüllerová, H., Saniga, M., Lu, M., Malamut, C., Seaton, D. B., Golub, L., Engell, A. J., Hill, S. W., & Lucas, R. 2011, "Structure and Dynamics of the 11 July 2010 Eclipse White-Light Corona," *ApJ*, **734**, 114

Pasachoff, J. M., Rušin, V., Saniga, M., Druckmüllerová, H., & Babcock, B. A. 2011, "Structure and Dynamics of the 2009 July 22 Eclipse White-Light Corona," *ApJ*, **742**, 29 doi: 10.1088/0004-637X/742/1/29

Pasachoff, J. M., Davis, A. B., Demianski, M., Lucas, R., Lu, M., Dantowitz, R., Rušin, V., Saniga, M., Seaton, D. B., Gaintatzis, P., Voulgaris, A., Seiradakis, J. H., Gary, D., Shaik, S. B. 2014, "Solar Activity and Motions in the Solar Chromosphere and Corona at the 2012 and 2013 Total and Annular Eclipses," 223rd AAS Meeting, National Harbor, MD, 118.01 2014AAS...22311801P

Pasachoff, J. M., Davis, A. B., Demianski, M., Rušin, V., Saniga, M., Seaton, D. B., Gaintatzis, P., Voulgaris, A., Lucas, R., Edwards, Z., Zeiler, M., & Kentrianakis, M. 2014, "Imaging and Spectra of the Chromosphere and Corona at the 2013 Total Eclipse in Gabon," Solar Physics Division/224th AAS Meeting, Boston, 323.16 2014AAS...22432316P

Pasachoff, J. M., 2015, "Preparing for and Observing the 2017 Total Solar Eclipse," Astronomical Society of the Pacific 2014 annual meeting, Burlingame, CA, 1E3, p. 26; in *Celebrating Science: Putting Education Best Practices to Work,* Greg Schultz, Sanlyn Busner, Linda Shore, and Jonathan Barnes, eds., pp. 43-49.

Pasachoff, J. M., Lu, M., Davis, A.B., Demianski, M., Rušin, V., Saniga, M., Seaton, D. B., Lucas, R., Babcock, B. A., Dantowitz, R., & Gaintatzis, P. 2014, "Coronal Dynamics at Recent Total Solar Eclipses," AGU (SH007) 17565, SH41B-4144 2014AGUFMSH41B4144P

Pasachoff, J. M., Rušin, V, Saniga, M,., Babcock, B. A., Lu, M., Davis, A. B., Dantowitz, R., Gaintatzis, J. H., Voulgaris, A., Seaton, D. B. & Shiota, K. 2015, "Structure and Dynamics of the 13/14 November 2012 White-Light Corona," *ApJ*, 800:90, 19 pp. doi:10.1088/0004-637X/800/2/90

Penn, M., Baer, B., and Isberner, F. 2015, "Citizen CATE Experiment: Prototype Testing and Plans," 34th Annual Symp Telescope Sci (Society for Astron. Sci., 2015, pp. 63-6; 2015SASS...34...63P)
https://sites.google.com/site/citizencateexperiment/,
http://www.noao.edu/noao/staff/mpenn/eclipse2017.html

Pevtsov, A. A. 2004, *Transequatorial Connections: Loops or Magnetic Separators? Multi-Wavelength Investigations of Solar Activity*, IAU Symp. 223. Edited by Alexander V. Stepanov, Elena E. Benevolenskaya, and Alexander G. Kosovichev. Cambridge, UK: Cambridge University Press, pp. 521-524
DOI 10.1017/S1743921304006726

Pishkalo, M.I. 2011, *Solar Phys.,* 270, 347.

Reale, F. 2014, *Living Rev. Solar Phys*., 11, 4
http://www.livingreviews.org/lrsp-2014-4
doi:10.12942/lrsp-2014-4

Rušin, V., & Rybanský, M. 1982, *Bull Astron. Inst. Czechoslavia*, 33, 219

Rušin, V., Druckmüller, M., Minarovech, M., & Saniga, M. 2008, *Astrophys. Space Sci*., 313, 345 2008Ap&SS.313..345R
DOI 10.1007/s10509-007-9686-2

Rušin, V., Druckmüller, M., Aniol, P., Minarovjech, M., Saniga, M., Mikic, Z., Linker, J. A., Lionello, R., Riley, P., & Titov, V. S. 2010, A&A, 513, A45 (7 pp.). 2010A&A...513A..45R

Rušin, V., Saniga, M., & Komžík, R. 2013, Contributions Astron. Obs. Skalnaté Pleso (CAOSP) 43, 73-80

Rušin, V., Saniga, M., & Komžík, R. 2014, Contributions Astron. Obs. Skalnaté Pleso (CAOSP) 44, 119-129

Tomczyk, S., Gallagher, D., Wu, Z, Zhang, H., Nelson, P., Burkepile, J., Kolinksi, D., & Sutherland, L. 2013, "The COronal Solar Magnetism Observatory (COSMO) Large Aperture Coronagraph," EGU General Assembly 2013, EGU2013-12573

http://adsabs.harvard.edu/abs/2013EGUGA..1512573T

Upton, L., & Hathaway, D. H. 2014, ApJ 780, 8pp

Vsekhsvjatsky, S. K., Dzubenko, N. I. Ivanchuk, V. I., & Rubo, G. A. 1970, "The structure of the solar corona on Sept. 22, 1968, from observations at Jurgamysh," Sol. Dannyje 9, 88 1970BSolD1970...88V

Usoskin, L. G., Arlt, R., Asvestari, E., Hawkins, E., Käpylä, M., Kovaltsov, G. A., Krivova, N., Lockwood, M., Mursula, K., O'Reilly, J., Owens, M., Scott, C. J., Sokoloff, D. D., Solanki, S. K., Soon, W., & Vaquero, J. M. 2015, A&A 581, A95(19 pp.) 2015A&A...581A..95U

Waldmeier, M. 1963, in The Solar Corona, edited by J. W. Evans, IAU Symposium No. 16, New York and London, 129.

Waldmeier, M. 1970, Astronomische Mitteilungen der Eidgenössichen Sternwarte Zürich, Nr. 299.

Webb, D. F., & Howard, T. A. 2012, Living Rev. Solar Phys., 9, 3 http://www.livingreviews.org/lrsp-2012-3